

On the nature of extra-framework aluminum species and improved catalytic properties in steamed zeolites

Authors: Konstantin Khivantsev,^{1†*} Nicholas R. Jaegers,^{1†*} Libor Kovarik,^{1†*} Miroslaw A. Derewinski,^{1,2} Ja-Hun Kwak^{3*} and Janos Szanyi^{1*}

Affiliations:

¹ Institute for Integrated Catalysis, Pacific Northwest National Laboratory, Richland, WA 99352, USA.

² Jerzy Haber Institute of Catalysis and Surface Chemistry, Polish Academy of Sciences, Krakow 30-239, Poland

³ Ulsan National Institute of Science and Technology (UNIST), South Korea.

* Correspondence to: K.K. Konstantin.Khivantsev@pnnl.gov . NRJ: NJaegers@gmail.com LK: Libor.Kovarik@pnnl.gov J.-H. K. E-mail: jhkwak@unist.ac.kr . J.Sz. E-mail: Janos.Szanyi@pnnl.gov;

† These authors contributed equally to the manuscript

Abstract: Steamed zeolites have improved catalytic properties for hydrocarbon activation (alkane cracking reaction as well as alkane dehydrogenation). The nature of this practically important phenomenon has remained a mystery for the last six decades and was speculated to be related to increased Bronsted acidity during dealumination. We now prove that during steaming aluminum oxide clusters evolve (due to hydrolysis of Al out of framework positions with the following clustering) in the zeolitic micropores with properties very similar to (nano)facets of hydroxylated transition-alumina surfaces. Bronsted acidity of zeolite does not increase and the total number of Bronsted acid sites decreases during steaming. O₅Al(VI)-OH surface sites of alumina clusters dehydroxylate at elevated temperatures to form penta-coordinate Al₁O₅ sites that are capable of initiating alkane cracking by breaking the first C-H bond very effectively, with the following reaction steps catalyzed by nearby zeolitic Bronsted acid sites. This explains the underlying reason behind the improved alkane cracking and alkane dehydrogenation activity of steamed zeolites: heterolytic C-H bond breaking occurs on penta Al(V)₁O₅ sites of aluminum oxide clusters confined in zeolitic pores. Furthermore, slightly decreased number of adjacent Al framework sites (due to Al dislodgement from the framework) decreases the coking activity, prolonging catalyst lifetime. Our findings explain the origin of enhanced activity of steamed zeolites at the molecular level and provide the missing understanding of the nature of extra-framework Al species formed in steamed/dealuminated zeolites. Furthermore, our findings suggest that similar La₂O₃ clusters exist for La-containing zeolites and the origin of their cracking activity promotion should be similar.

Zeolites are arguably the most important industrial materials employed in petroleum refining and cracking [1-9]. They are crystalline and microporous solids composed of tetrahedral SiO₄ and Si-OH-Al units, with ordered arrays of micropores/microcavities: alkane transformations into more

valuable chemicals take place in zeolitic pores at high temperatures 400-650 °C. Together with transition aluminas, zeolites are mass-produced industrially, millions of tons every year [1-9]. For hydrocarbon cracking, it is known that mild steaming zeolites at elevated temperatures in the presence of water steam significantly improves their cracking activity and prolongs their lifetime [1-9]. This phenomenon has remained a mystery for the last six decades. It is generally known that steaming generates extra-framework Al (EFAL) species whose nature is not known, and it is often speculated that because of generation of EFAL species Bronsted acidity of zeolites somehow increases contributing to increased protolytic cracking activity [10]. Despite that, comprehensive reviews of the literature conclude that no convincing evidence exists of increased Bronsted acidity after mild hydrothermal treatment [11].

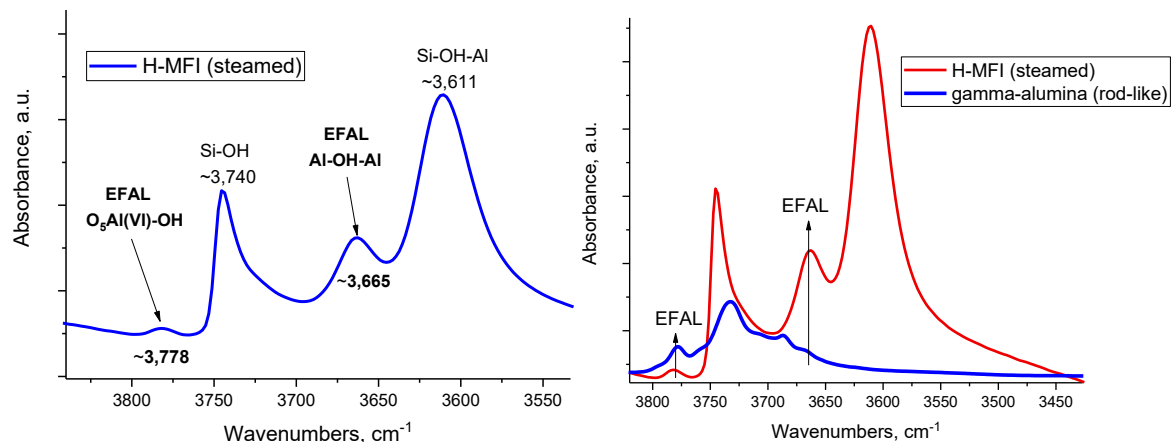
Previously, we solved a century-old old mystery of gamma-alumina surface properties and surface OH group assignments [12] on the surface of transition (gamma) alumina. More specifically, we found that the OH bands ~3,770-3,780 belong to amphoteric O₅Al(VI)-OH sites associated with most stable (100) facets and (100) nano-segments of restructured (110) surfaces [*(110) surfaces of gamma-alumina restructure into (100) and (111) nano-segments; as such, although macroscopically defined (110) surface exists, its atomic-level view in fact shows that it is completely broken into (100) and (110) nano-segments, due to higher thermodynamic stability of (100) and (111) facets; this holds true for nanosized commercial high-surface area (up 200 m²/g) SBA-200 gamma-alumina as well as larger and well-defined rhombus-platelet gamma-alumina crystals; Figs. S1,S2*].

As we showed [12], the OH bands between 3,720-3,740 cm⁻¹ belong to tetrahedral O₃Al-OH sites. Bands below 3,690 cm⁻¹ belong to weakly acidic doubly and triply-bridging OH groups [Al-OH-Al] of gamma-alumina [12]. We also determined that alcohol dehydration catalytic activity stems from the presence of O₅Al(VI)-OH sites [12]. Upon thermal dehydroxylation, O₅Al-OH sites transform into coordinatively unsaturated O₅Al sites that can coordinate N₂ and CO.

This new understanding allows us to finally determine the nature of extra-framework Al species formed in zeolites which has not been possible before. More specifically, commonly for all zeolites H-SSZ-13, H-ZSM-5 and H-BEA zeolites upon mild steaming all produce the following signatures of extra-framework species: bands in the -OH stretching region at ~3,770-3,780 cm⁻¹, bands in the ~3,660-3,640 cm⁻¹ (Fig. S3). The 3,770-3,780 cm⁻¹ band is often ignored because it is somewhat less intense and present as a tail on Si-OH groups [13]. The comparison between the signatures of

OH groups on the surface of gamma-alumina and mildly steamed zeolites is striking and immediately suggests that the EFAL species formed in zeolites have very similar OH bands as transition-alumina surfaces

(Fig. 1).



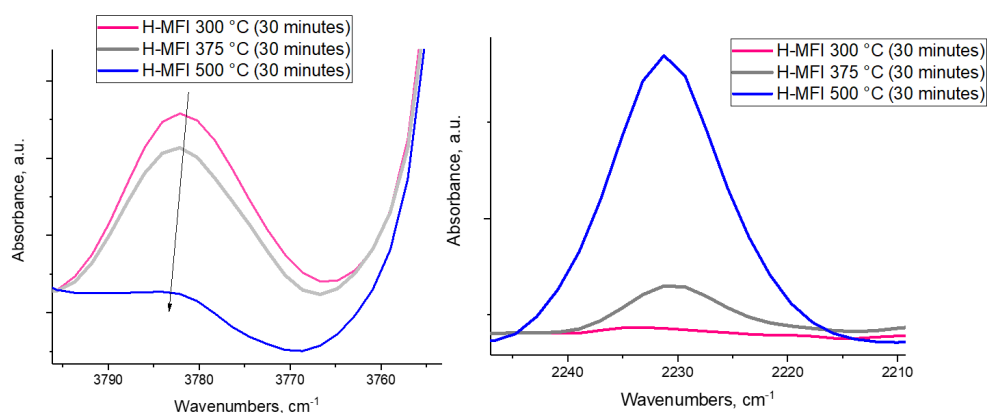
5

Figure 1. A. FTIR spectrum of the OH region of steamed H-MFI sample. B. FTIR spectrum comparison of the OH regions of steamed H-MFI and rod-like gamma-alumina sample.

O_3Al-OH bands ($\sim 3,720-3,740$) are obscured by the intense O_3Si-OH band of zeolite.

10

We now prove that EFAL species in zeolite are in fact aluminum oxide clusters (formed in zeolite upon steaming) and they have similar surface properties as typical nano-segmented aluminum, oxide surfaces. As we heat the steamed H-MFI sample above ~ 400 °C, the $\sim 3,780$ cm^{-1} OH band goes down (Fig. 2).



15

Figure 2. Steamed H-MFI sample (all spectra were collected on the same pellet) **A (left spectrum)**: FTIR of the OH region showing the diminishing of the $\sim 3,780$ cm^{-1} band with temperature (spectra were recorded at room temperature). **B (right spectrum)**: FTIR final spectra collected after introducing a total 1 Torr of CO (total pressure; room temperature) on the steamed H-MFI sample after each thermal treatment. How exactly the Al(V)-CO spectra develop sequentially during in-situ N_2 and CO adsorption is shown in Figure 4.

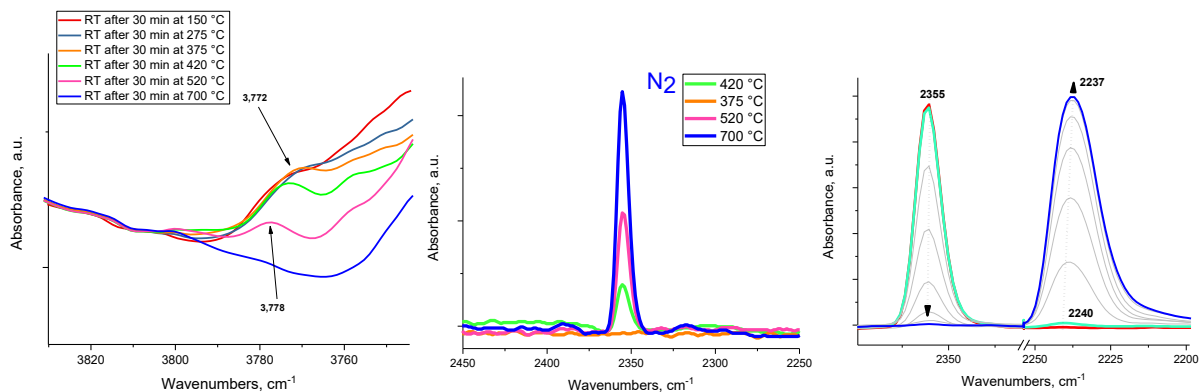


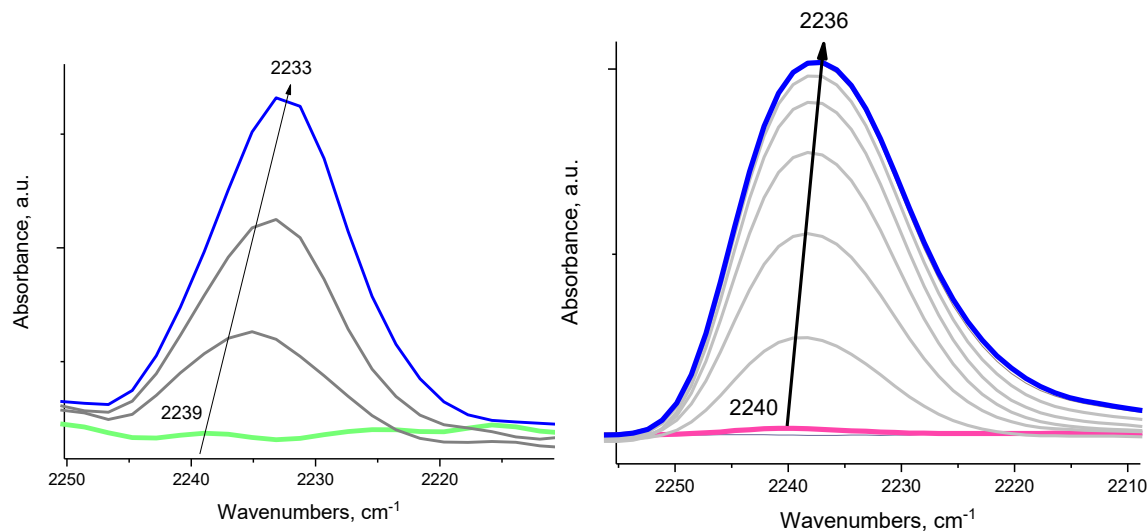
Figure 3. Rhombus-platelet gamma-alumina sample **A (left spectrum)**: FTIR of the OH region showing the diminishing of the $\sim 3,780\text{ cm}^{-1}$ band with temperature (spectra were recorded at room temperature after each treatment). **B (middle spectrum)**: FTIR spectra collected after introducing a total 5 Torr of nitrogen (total pressure; room temperature) on the alumina sample after each thermal treatment: evolution of the N-N stretching band is due to N_2 adsorption on Al_1O_5 dehydroxylated sites (it occurs only when the specific OH band goes down and dehydroxylation takes place). **C (right spectrum)**: Sequential CO adsorption on the sample containing $\text{O}_5\text{Al-N}_2$ complex: this establishes that CO displaces N_2 as a coordination site in $\text{O}_5\text{Al-CO}$ complex (this complex has CO stretch around $\sim 2,240\text{-}2,236\text{ cm}^{-1}$, similarly to the surface Al_1O_5 sites of dehydroxylated Al_2O_3 clusters in zeolites. Please note that the spectra of dehydroxylation for SBA-200 alumina sample and rod-like alumina sample are shown in **Figs. S4**.

Simultaneously, coordinatively unsaturated penta Al site is produced – we probe it with CO adsorption using Infra-Red spectroscopy. CO adsorption on the steamed (*and not thermally dehydroxylated after steaming*) ZSM-5 sample (where $3,780\text{ cm}^{-1}$ band is not diminished) does not lead to significant CO or N_2 adsorption (**Fig. 2**). Exactly the same phenomenon is observed for various alumina samples (**Fig. 3**, **Fig. S4**): as $3,778\text{ cm}^{-1}$ band goes down (note that the location of this band is very close both for alumina (100) segments and steamed zeolite), the $\sim 2,233\text{-}2,236\text{ cm}^{-1}$ band develops after CO adsorption (**Fig. 2**). This band is in essentially the same position as the one seen for transition alumina surfaces. Moreover, it grows in a similar fashion both for dehydroxylated alumina surfaces and dehydroxylated zeolite (**Fig. 4**).

Also, note that N_2 adsorption on dehydroxylated Al_2O_3 clusters in zeolites also produces the N-N stretch at $\sim 2,353\text{ cm}^{-1}$ at room temperature analogously to N_2 adsorption on transition-alumina surface $\sim 2,256\text{ cm}^{-1}$ band.

The more Al-OH site is dehydroxylated, the more intense the band of Al-CO complex at $2,239\text{ cm}^{-1}$ [12], which is identical to gamma-alumina. Thus, we establish equivalency between hydroxylated EFAL species and hydroxylated (100) alumina segments that dehydroxylate with the formation of coordinatively unsaturated Al_1O_5 sites. This is the direct evidence of the fact that the

hydrated Al_2O_3 clusters that are formed in zeolite have similar Al-OH sites as the ones seen on transition (gamma) alumina surface. They also dehydroxylate similarly producing coordinatively unsaturated Al_1O_5 sites with similar coordination/chemisorption properties (Fig. 4).



5 Figure 4. **A (left spectrum):** FTIR during sequential CO adsorption (~ 1 Torr) on steamed H-MFI sample after dehydroxylation at 500°C . **B (right spectrum):** FTIR during sequential CO adsorption (~ 1 Torr) on rod-like gamma-alumina sample after dehydroxylation at 500°C .

10 The alumina clusters thus formed are limited in size by the zeolite dimensions (< 1 nm): due to this, they must consist of majorly surface sites and not bulk. Therefore, now we can explain the high fraction of penta-sites observed in steamed zeolites with NMR (Fig. S5). We previously showed that penta Al sites are located majorly on (100) segments and nano-segments of gamma-alumina (Fig. S1,S2 TEM images) [12]: those segments can be as “small” as a few atoms (Figs. S1,S2). Regular alumina samples contain majority of atoms in the bulk (tetra and octahedral Al sites): even alumina samples with relatively high surface area contain below a few percent of penta-Al sites (Fig. S6), reflected by the low contribution of the surface to the total number of Al sites. Remarkably, Al_2O_3 clusters in zeolites (due to their very small nano-sized nature) consist majorly of surface sites with the increased fraction of Al_1O_5 sites (after dehydroxylation) and $\text{O}_5\text{Al(VI)-OH}$ sites (before dehydroxylation). Simultaneously, in steamed H-MFI Al tetra- and octa- sites broaden and develop (octa) compared with H-MFI, consistent with alumina cluster formation.

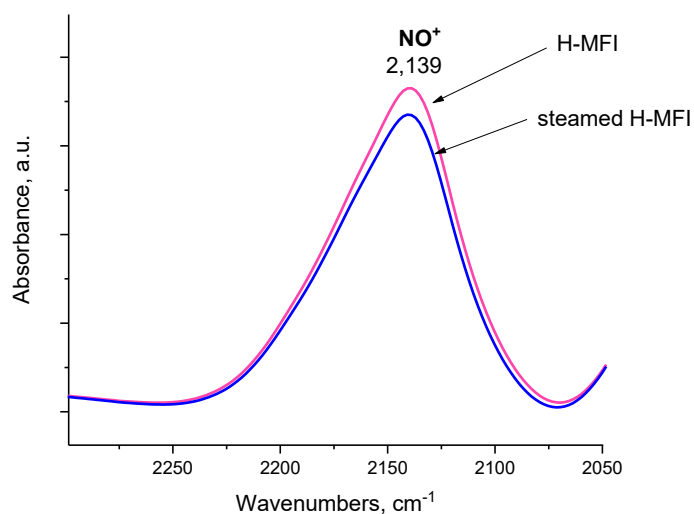
20 As moderate steaming removes some framework Al sites and produces extra-framework alumina clusters (identified herein unambiguously) enriched with surface Al_1O_5 sites (after thermal

dehydroxylation), the propane cracking activity increases dramatically (~6 times) (Table 1), suggesting that the presence of extra-framework alumina clusters is critical for improving cracking activity. Concomitantly, alkane dehydrogenation activity increases (Table 1).

5 Table 1. Propane cracking and dehydrogenation activity comparison of different samples. WHSV ~ 20 hr⁻¹. Note that cracking produces methane and ethylene, whereas dehydrogenation produces propylene.

Sample	Cracking activity (methane plus ethylene)*10 ⁷ moles/g*s; 500 °C	Dehydrogenation activity (propylene) 10 ⁷ moles/g*s; 500 °C
H-MFI	1.4	1.1
H-MFI steamed (dehydroxylated)	9.3	4.5
Rhombus-platelet gamma-alumina	0.1	0.8

10 Furthermore, probing Bronsted acid sites by replacing H⁺ with NO⁺ ions with IR active N-O stretch [18,19], shows decrease of the number of Bronsted acid sites and no increase in acid strength (Fig. 5). Therefore, despite the decrease in the Bronsted acid sites and no change in their acidity, the alkane C-H activation activity increases dramatically due to presence of Al₂O₃ clusters.



15 Figure 5. FTIR spectra in the N-O stretching region: comparison of parent H-MFI (containing no EFAL) and steamed H-MFI (containing EFAL). NO⁺ was produced by NO₂ adsorption (0.5 Torr in total). Because NO⁺ occupies H sites, it is a direct measure

of changes in Bronsted acid amount and acidity. It is clear that total number of Bronsted acid sites decreases after steaming (peak area is lower), with no evidence of increased Bronsted acidity (no shift in the NO^+ stretch).

Thus, it becomes clear that Al_2O_3 clusters form and due to their presence, cracking activity increases. How can alumina clusters with enriched Al_1O_5 sites help this process? We show spectroscopically (Fig. 6), that dehydroxylated $\text{O}_5\text{Al(VI)-OH}$ sites are capable of heterolytically breaking the C-H bond of methane (hydrocarbon with the most inert bonds and the hardest to activate) at temperatures as low as 200 °C, as well as for other saturated hydrocarbons such as octane.

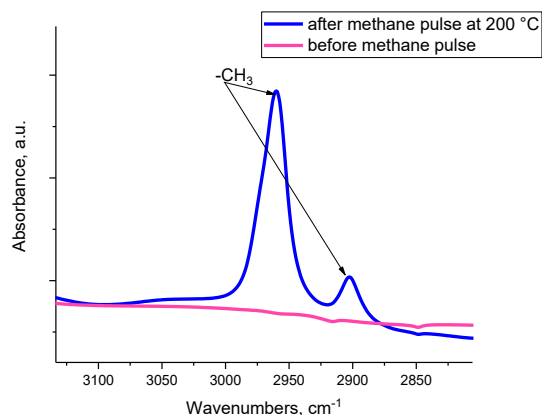


Figure 6. FTIR spectra showing the C-H stretching region of dehydroxylated gamma-alumina before and after methane pulse (~0.5 Torr total pressure of methane) at 200 °C. The bands that grow correspond to two IR active vibrations of methyl group.

Please note, that when the $\text{O}_5\text{Al(VI)-OH}$ sites are not dehydroxylated by thermal pre-treatment at high temperature, basically no activity is observed for activation of C-H bonds (Fig. S7).

It becomes clear that when -OH groups on AlO_5 sites are present, no C-H bond breaking occurs at temperatures when site dehydroxylation is not possible, and only when Al_1O_5 form upon thermal dehydroxylation, heterolytic C-H bond breaking occurs with the formation of methyl fragment, identified by us spectroscopically (Fig. 6):



For propane, the first step is: $\text{C}_3\text{H}_8 + \text{O}_4\text{Al-O-Al} \rightarrow \text{CH}_3\text{-CH}_2\text{-CH}_2\text{-AlO}_4\text{--OH--Al}$. (Please note in that scheme Al_1O_5 is denoted as $\text{O}_4\text{Al-O-Al}$ to better show the presence of Al-O-Al bonds)

Beta-hydride elimination on Al-propyl fragment produces propylene (C₃H₆) and Al hydride species:



5

Hydridic hydrogen then recombines with the acidic hydrogen of the (bridging) OH group to reform the Al₁O₅ site and molecular hydrogen:



10

Further reaction steps (leading to cracking products) then occur on Bronsted acid sites, located in the vicinity of alumina clusters: Si-O(Alkyl)-Al species form from reaction of olefin with Bronsted acid sites:

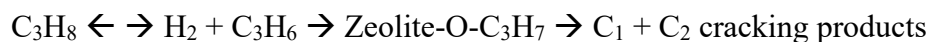


15

This step is critical to form the alkoxy intermediate required for cracking! Once alkoxy species are formed, they can irreversibly crack on Bronsted acid sites.

This finding suggests the following reaction sequence: since propane dehydrogenation reaction is reversible: $\text{C}_3\text{H}_8 \leftarrow \rightarrow \text{C}_3\text{H}_6 + \text{H}_2$, the reaction is limited by the equilibrium: however, because of proximity of Al₂O₃ clusters to zeolite acid sites, once propylene forms, it can immediately participate in further irreversible reactions on Bronsted acid sites (leading to cracking products): thus, propylene is continuously removed shifting equilibrium of the reversible first reaction to the right, increasing propane conversion:

20



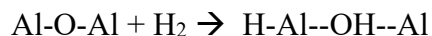
25

Indeed, notably, even for regular gamma-alumina we observe that it can convert propane at 500 °C to propylene and hydrogen ([Table 1](#)) (please note it also can perform the microscopic reverse of this reaction: propylene hydrogenation to propane, showing that hydrogenation and dehydrogenation occur via the same intermediate). Dehydrogenation selectivity of gamma-alumina is ~90%. Remarkably, it has ~10% cracking selectivity to CH₄ and C₂H₄ in ratio almost 1:1 (with minor ethane amounts due to some back-hydrogenation of ethylene to ethane). Thus, Al₁O₅ are essential for observing this activity both on gamma-alumina and zeolite. The

30

cracking/dehydrogenation catalytic reactivity on zeolite is thus due to presence of Al_2O_3 clusters with coordinatively unsaturated Al_1O_5 sites next to zeolitic Bronsted acid sites.

Furthermore, based on this mechanism, the aluminum hydride species should form on Al_2O_3 clusters and *Al-H species are the essential intermediates in olefin hydrogenation and alkane activation reactions*. Indeed, treatment with H_2 (Fig. S8) or D_2 (Fig. 7) produces Al-H and Al-D stretches on gamma-alumina with H/D isotopic shift fully consistent with hydride formation. Please, note that hydrides can form on different Al-O sites, not necessarily on Al_1O_5 site (C-H breaking, however, seems to occur on dehydroxylated coordinatively unsaturated Al-O sites of aluminum oxide clusters):



In steamed zeolites, remarkably, D_2 treatment leads to the formation of hydrides with essentially the same Al-D stretching frequencies, as the ones observed on gamma-alumina, fully consistent with our findings: this is the first observation of aluminum hydride species in steamed zeolites.

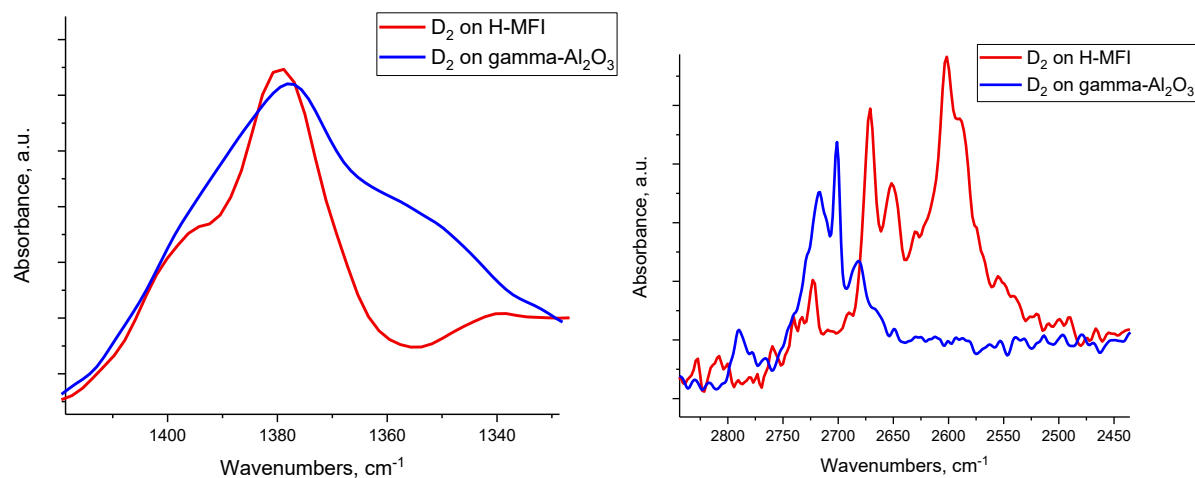
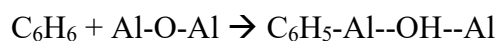


Figure 7. FTIR spectra in the Al-D (left graph) and O-D (right graph) stretching regions after D_2 treatment of steamed H-MFI and gamma-alumina. Both samples were pre-treated at 500 °C prior to reaction with D_2 .

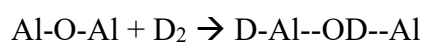
We also note, looking at cracking rates, that the presence of water (i.e.m OH groups) on extra-framework Al_1O_5 sites is detrimental, as the activity decreases significantly (at temperatures when -OH dehydroxylation did not take place) (Table 1). This further highlights the critical role of

dehydroxylated Al₁O₅ sites located on alumina clusters formed upon steaming. This also explains, why at lower temperatures, presence of O₅Al(VI)-OH sites with -OH group (dissociated water) is detrimental for alkane transformation activity (because those sites are covered by -OH groups and cannot thus provide C-H bond breaking).

5 With this insight, we can now explain the previously unexplained findings in the literature that steamed zeolites can effectively catalyze H₂+D₂ exchange (to form HD), as well as (benzene/hydrocarbons +D₂) exchange to form deuterated hydrocarbons (at elevated temperatures) [14,15]. Previously, it has been suggested to be a zeolitic Bronsted-acid catalyzed process: our new findings suggest this view is not correct because zeolites with little EFAL have very little activity for (benzene+D₂) exchange. Only when EFAL species are present (which we have now shown are, in fact, Al₂O₃ clusters), this process occurs. It now becomes clear how this process takes place: hydrocarbons dissociate on coordinatively unsaturated Al-O sites (Fig. 6) (this example is for benzene):

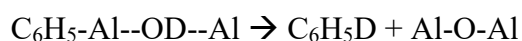


15 D₂ gets incorporated onto alumina surface via activation on various Al-O sites (Fig. 7):



Because bridging protons are weakly acidic [12]: they can move/"hop" between different acidic hydroxyls (in the presence of very minor moisture amounts this hopping process becomes much easier which explains some literature data suggesting that in steamed zeolites in the presence of minute moisture amounts H/D exchange in benzene is faster [20]):

20 H in OH group then can exchange for D next to Al-C₆H₅ site via the above-described proton-hopping mechanism. After that, deuterated benzene evolves:



25 Essentially the same process can occur on gamma-alumina surface as well (see Fig. S9 confirming HD formation from (H₂+D₂) reaction on rhombus platelet gamma-alumina).

In summary, we have solved the 50-year-old mystery for the largest scale heterogeneous zeolite catalytic process: controlled steaming increases cracking activity of zeolites due to the formation of alumina clusters enriched with Al(V)₁O₅ surface sites in zeolite micropores. These sites facilitate facile alkane C-H bond breaking events in zeolite much more effectively than in their

absence. Simultaneously, Bronsted acid Al-OH-Si site density decreases: this *slight* decrease is also beneficial because coke formation is favored by proximity of many Bronsted acid sites, and some optimal density of these Bronsted acid site exists that decreases coke formation (mesopore formation would also facilitate diffusion of those species before they form “real” coke). As long as not too much Al is removed from the framework and enough Al₂O₃ clusters are formed, the presence of Al₁O₅ on their surface leads to easier C-H bond breaking events for cracking and dehydrogenation reaction. Our findings further suggest that La-promotion of cracking activity in zeolites is also related to the formation of La₂O₃ clusters in the zeolitic micropores – once dehydroxylated, these clusters possess coordinatively unsaturated La-O sites, facilitating C-H bond breaking events.

Our study also suggests that most likely no NMR “invisible” tri-coordinate Al species exist in mildly steamed zeolites (or on alumina surface) in measurable amounts. We have already shown that in some previous studies spectroscopic signatures were previously incorrectly attributed to NMR-“invisible” tricoordinate Al sites on the surface of transition aluminas – we showed that those in fact belonged to penta-Al sites [12]. The formation of tri-coordinate Al sites was additionally suggested previously for some steamed zeolites [15] on the basis of Al K-edge EXAFS modeling – the corroborating evidence for the formation of these sites was speculated to be CO adsorption on those “Al₁O₃” sites producing CO adsorption infrared band around ~2,230 cm⁻¹. We showed convincingly that this band belongs to penta-Al sites and is not associated with 3-coordinate Al sites. Furthermore, some recent studies took this concept even further and explained the enhanced alcohol dehydration activity in steamed zeolites by the presence of extra-framework tri-coordinate Al sites: this is obviously incorrect. We herein attribute enhanced activity in alcohol dehydration for steamed zeolites to the presence of hydroxylated alumina clusters with abundant O₅Al(VI)-OH sites that are the true active sites for alcohol dehydration [12]. Furthermore, studies that claimed the presence of 3-coordinate Al sites in steamed zeolites as probed by NMR spectroscopy with P(CH₃)₃ and O=P(CH₃)₃ probe molecules should be critically re-assessed: the signature ascribed to tri-coordinate Al sites in those studies most likely belong to strongly Lewis acidic Al(V) sites [12,17].

References

- (1) H. Heinemann, "Development of Industrial Catalysis," Handbook of Heterogeneous Catalysis. Wiley-Verlag Chemie: Weinheim. 1997.
- (2) Sachtler W.M.H. (2002) Catalysis from Art to Science. In: Carley A.F., Davies P.R., Hutchings G.J., Spencer M.S. (eds) Surface Chemistry and Catalysis. Fundamental and Applied Catalysis. Springer, Boston, MA
- 5 (3) W.O. Haag, R.M. Dessau, Proceedings Intern. Congress Catal. in Berlin, Germany, Vol II, p. 305. Dechema-Verlag: Frankfurt am Main, Germany. 1984.
- (4) D. W. Breck, US Pat., 3,130,007, 1964.
- (5) N. Rahimi, R. Karimzadeh, Applied Catalysis A: General 398 (2011) 1-17
- (6) R. J. Argauer, G. R. Landolt, US Pat., 3,702,886, 1972.
- 10 (7) P. B. Venuto, T. E. Habib, Fluid catalytic cracking with zeolite catalysts, Marcel Dekker, New York, 1979.
- (8) J. Scherzer, Octane-Enhancing Zeolitic FCC Catalysts: Scientific and Technical Aspects, Marcel Dekker, New York, 1990
- (9) D. W. Breck and E. M. Flanigen, Molecular Sieves, London, 1968, p. 47.
- (10) J. Haw, Phys. Chem. Chem. Phys., 2002, 4, 5431-5441
- 15 (11) S.M. Babitz, B.A. Williams, J.T. Miller, R.Q. Snurr, W.O. Haag, H.H Kung, Applied Catalysis A: General 179 (1999) 71-86
- (12) K. Khivantsev, N. R. Jaegers, J.-H. Kwak, J. Szanyi, L. Kovarik, Angew. Chem. Int. Ed. 2021, 60, 2 - 11
- (13) J. Szanyi, M.T. Paffett, Microporous Materials 7 (1996) 201-218
- (14) Kramer, G. J.; van Santen, R. A.; Erneis, C. A.; Nowak, A. K. Nature, 1993, 363, 529-31.
- 20 (15) Kramer, G. J.; van Santen, R. A. J. Am. Chem. Soc. 1995 117 1766-76.
- (16) J. A. van Bokhoven, A. M. J. van der Eerden, D. C. Koningsberger, J. Am. Chem. Soc. 2003, 125, 7435-7442
- (17) J.-P. Gilson, G. C. Edwards, A. W. Peters, K. Rajagopalan, R. F. Wormsbecher, T. G. Roberie, M. P. Shatlock. Chem. Soc., Chem. Commun., 1987 91-92
- (18) Khivantsev, K., Jaegers, N.R., Kovarik, L. et al. Emiss. Control Sci. Technol. 6, 126-138 (2020).
- 25 (19) K. Hadjiivanov, Catalysis Reviews 2000 42 (1-2), 71-144

Acknowledgments:

The research described in paper is part of the Quickstarter Initiative at Pacific Northwest National Laboratory. It was conducted under the Laboratory Directed Research and Development Program at PNNL, a multiprogram national laboratory operated by Battelle for the U.S. Department of Energy (DOE) under Contract DE-AC05-76RL01830. The research described in this paper was performed in the Environmental Molecular Sciences Laboratory (EMSL), a national scientific user facility sponsored by the DOE's Office of Biological and Environmental Research. This work was supported by US Department of Energy, Office of Science, Office of Basic Energy Sciences, Division of Chemical Sciences, Biosciences, and Geosciences.

30

35

Competing interests: Authors have no conflicts to declare.

Data and materials availability: All data is available in the main text or the supplementary materials.

40

5

Supporting Information:

On the nature of extra-framework aluminum species and improved catalytic properties in steamed zeolites

Authors: Konstantin Khivantsev,^{1†*} Nicholas R. Jaegers,^{1*} Mirosław A. Derewinski,^{1,2} Libor Kovarik,^{1†} Ja-Hun Kwak^{3*} and Janos Szanyi^{1†*}

Affiliations:

¹ Institute for Integrated Catalysis, Pacific Northwest National Laboratory, Richland, WA 99352, USA.

² Jerzy Haber Institute of Catalysis and Surface Chemistry, Polish Academy of Sciences, Krakow 30-239, Poland

³ Ulsan National Institute of Science and Technology (UNIST), South Korea.

* Correspondence to: K.K. Konstantin.Khivantsev@pnnl.gov . NRJ: njaegers@gmail.com LL: Libor.Kovarik@pnnl.gov J.-H. K. E-mail: jhkwak@unist.ac.kr . J.Sz. E-mail: Janos.Szanyi@pnnl.gov;

† These authors contributed equally to the manuscript

Materials and methods

MFI sample in the ammonium form with Si/Al ratio ~ 15 was supplied by Zeolyst. First, this sample was calcined in the dry air flow at 550 °C for 5 hours to remove ammonia. The sample was subsequently subjected to treatment with the ~0.1 M solution of ammonium hexafluorosilicate (99.999%, sigma

aldrich) under continuous stirring for 15 minutes at 80 °C. The powder was then centrifuged and washed multiple times with DI water. The zeolite cake was then dried under N₂ flow in the furnace at ~100 °C, and subsequently calcined at 550 °C for 3 hours in the flow of dry air. This produced the H-MFI sample titled “H-MFI” for our experiments.

5 To produce the steamed H-MFI sample (containing extra-framework Al species), H-MFI was subjected to steam treatment at 420 °C in the flow-through quartz reactor with air flow through the water saturator for 30 minutes. The sample was cooled down in the flow of wet air to 200 °C, and then held at 200 °C in the flow of dry air for 1 hour before cooling. This sample is called “steamed H-MFI”.

10 Other H-zeolites were steamed using similar method, such as H-SSZ-13 and H-BEA (their infrared spectra are shown in Fig. S2).

Rhombus-platelet γ -alumina used was synthesized from aluminum isopropoxide via a hydrolysis method (ref 12). More specifically, approximately 10 g of aluminum isopropoxide was added to ~50 mL of water with vigorous stirring at 80 °C for 1 h. The mixture was transferred to the 125 mL Teflon liner of a Parr reactor and placed into an oven and kept at 200 °C for 24 h. After cooling to room temperature, the powder was collected by filtration, washed with distilled water, and dried at 100 °C. The as-synthesized boehmite powder was then calcined at 800 °C for 2 h to convert it to rhombus-platelet γ -alumina with surface area of approximately 70 m²/g.

20 Commercial SBA-200 γ -alumina with surface area ~ 200 m²/g was used without additional pretreatment.

Rod-like γ -alumina (with surface area ~70 m²/g) was synthesized according to the previous method at the pH ~ 4 (ref 12).

25 The *in-situ* static transmission IR experiments were conducted in a home-built cell housed in the sample compartment of a Bruker Vertex 80 spectrometer, equipped with an MCT detector and operated at 4 cm⁻¹ resolution. The powder sample was pressed onto a tungsten mesh which, in turn, was mounted onto a copper heating assembly attached to a ceramic feedthrough. The sample could be resistively heated, and the sample temperature was monitored by a thermocouple spot welded onto the top center of the W grid. The cold finger on the glass bulb containing CO (99.995%) was cooled with liquid nitrogen to eliminate any contamination originating from metal carbonyls, while NO₂ (99.9 %) was cleaned with multiple freeze–pump–thaw cycles. Research-grade methane (purity

30

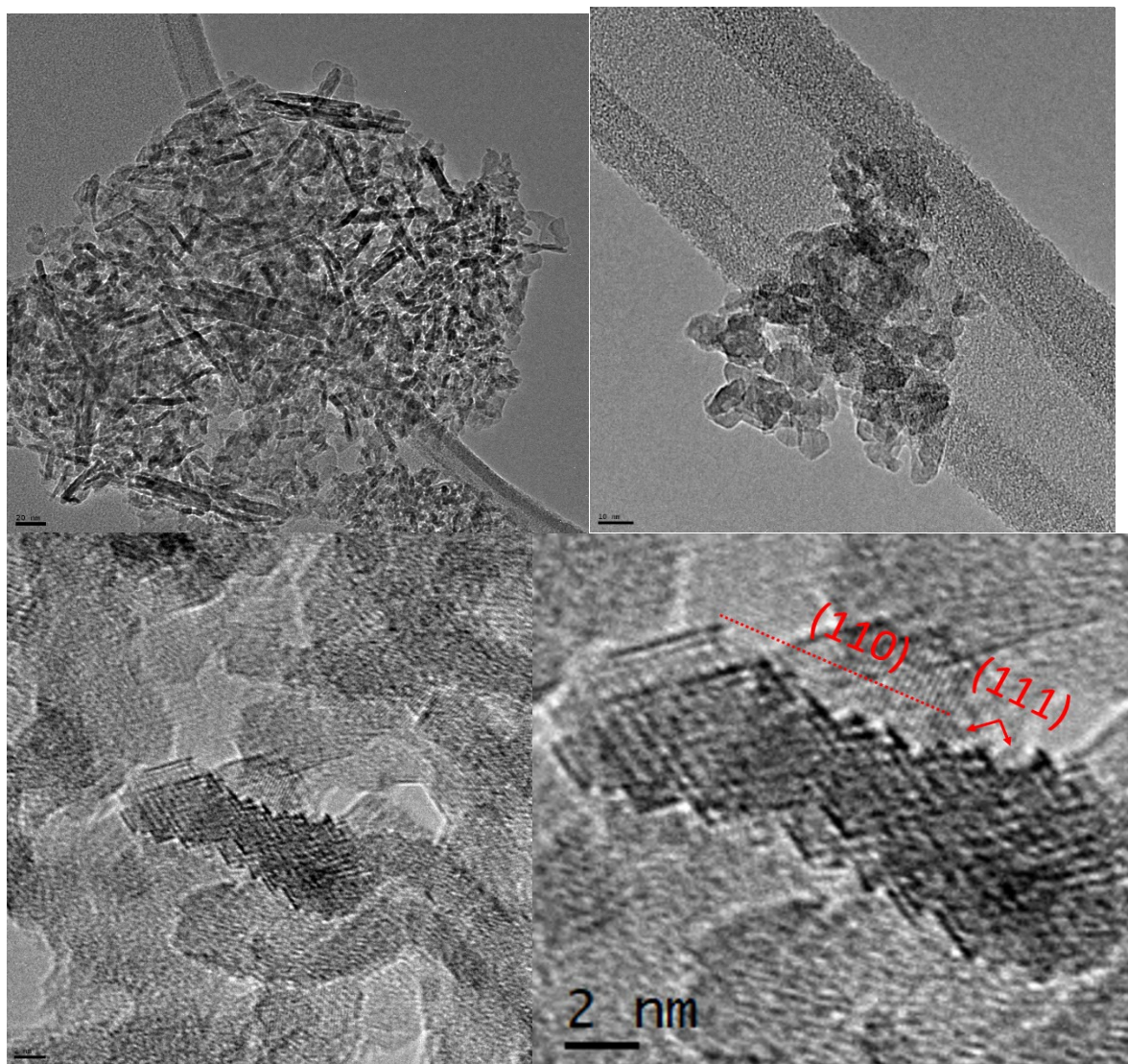
99.995%) was used. Octane (anhydrous, 99.99% sigma-aldrich) was purified with multiple freeze-pump-thaw cycles and stored in a glass bulb. D₂ was purchased from Cambridge Isotopes, it was contained in a glass bulb and purified with liquid nitrogen trap to remove moisture traces. Research-grade H₂ was used (99.995% purity).

5 Microscopy analysis was performed with a FEI Titan 80-300 microscope operated at 300 kV. The instrument is equipped with a CEOS GmbH double-hexapole aberration corrector for the probe-forming lens, which allows for imaging with 0.1 nm resolution in scanning transmission electron microscopy mode (STEM). HAADF-STEM images were acquired with a high angle annular dark field (HAADF) detector with inner collection angle set to 52 mrad.

10 ²⁷Al MAS NMR measurements were performed at room temperature on a Bruker 850 MHz NMR spectrometer, operating at a magnetic field of 19.975 T. The corresponding ²⁷Al Larmor frequency is 221.4125 MHz. A single pulse sequence comprised of a $\pi/9$ pulse width of 0.3 μ s, a recycle delay of 2 s, and an acquisition time of 30 ms was employed to collect the free induction decays (FID). To enhance the intensity of the observed spectral features over the noise, 4,096
15 repetitions were employed for each FID. Each collected FID was subsequently Fourier Transformed to the frequency domain where both zero and first order phase corrections were applied. The broad spectrometer background signal was collected with a sample containing no Al species under the same conditions and subsequently subtracted from each Al spectra. The data were simulated for best fit and the intensities of each coordination environment from the
20 simulations were taken together to provide the fractional abundance. Total intensity was normalized to the carefully measured mass of each sample used for the NMR experiment, which was typically ~ 15 mg. All NMR data were acquired at a sample spinning rate of 18.7 kHz (\pm 5 Hz) and externally referenced to 1.0 M aqueous Al(NO₃)₃ (0 ppm). The samples were packed inside 3.2 mm pencil-type NMR rotors. The rotors were subsequently sealed and placed in vials
25 until transported to the NMR probe.

 Catalytic experiments were performed in the quartz flow-through reactor. 75 mg of catalyst powder was loaded in the reactor and thermally pre-treated in the flow of dry air at 500 °C, and then purged with dry Helium at this temperature for 30 minutes (reactions at 390 °C were also performed: in this case, the temperature was quickly ramped to the desired temperature (390 °C)
30 and catalytic activity was tested at this temperature). UHP 2% Propane in He gas mixture was

used. WHSV was $\sim 20 \text{ hr}^{-1}$. Products were quantified with gas chromatography with FID detector. Propane conversions were $< 2\%$. Reaction was performed at temperatures $500 \text{ }^\circ\text{C}$ and $400 \text{ }^\circ\text{C}$.



5 Figure S1. typical HRTEM images of high surface area ($\sim 200 \text{ m}^2/\text{g}$) SBA-200 γ -alumina sample. It consists of abundant platelets can be easily seen (image 1) as well less common less well-defined nanocrystal shapes (image 2). Image 3 shows nanocrystal of SBA-200 with macroscopically defined (110) surface: image 4 shows magnified nanocrystal showing that (110) facet is reconstructed into (111) and (100) ridges, completely analogous to all gamma-alumina surfaces.

10

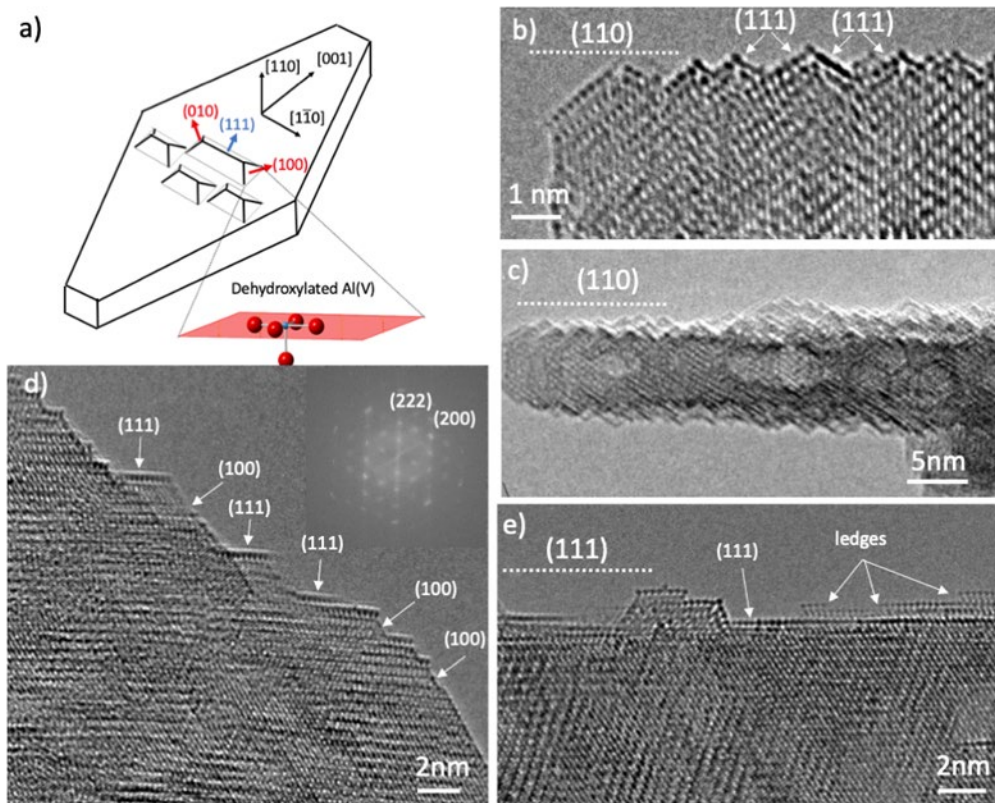


Figure S2. A). Schematic of rhombus-platelet alumina crystals showing reconstruction of (110) surface into (100 and (111) nano-segments. B)-C). Atomically resolved HRTEM image (110) surfaces of rhombus-platelet γ -alumina. The (110) surface is reconstructed into (111) and (100) facets. This is typical for all gamma-alumina samples. D). HRTEM observation of an irrational surface of γ -alumina showing that it also contains (100) and (111) nano-segments. (e) HRTEM image of (111) surface facet.

5

10

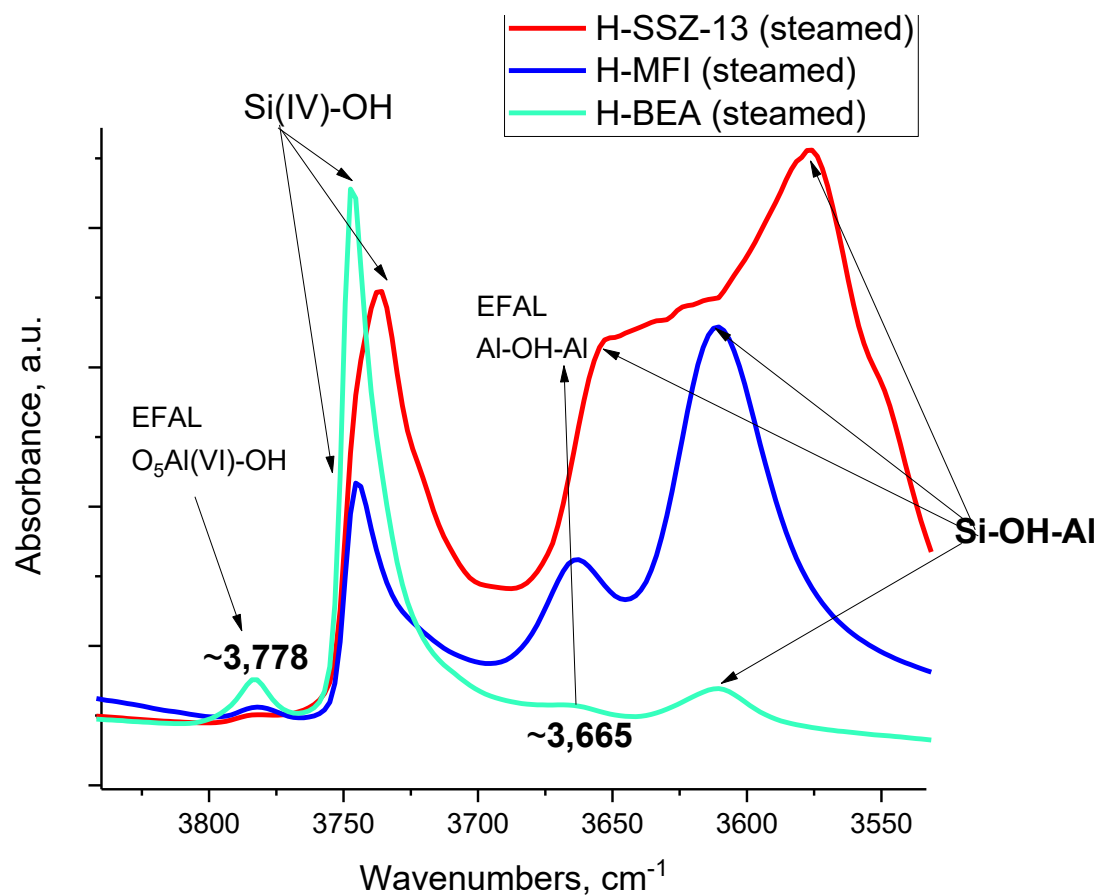


Figure S3. FTIR of the OH region of steamed H-SSZ-13, H-BEA and H-MFI samples showing similar EFAL features for all of them.

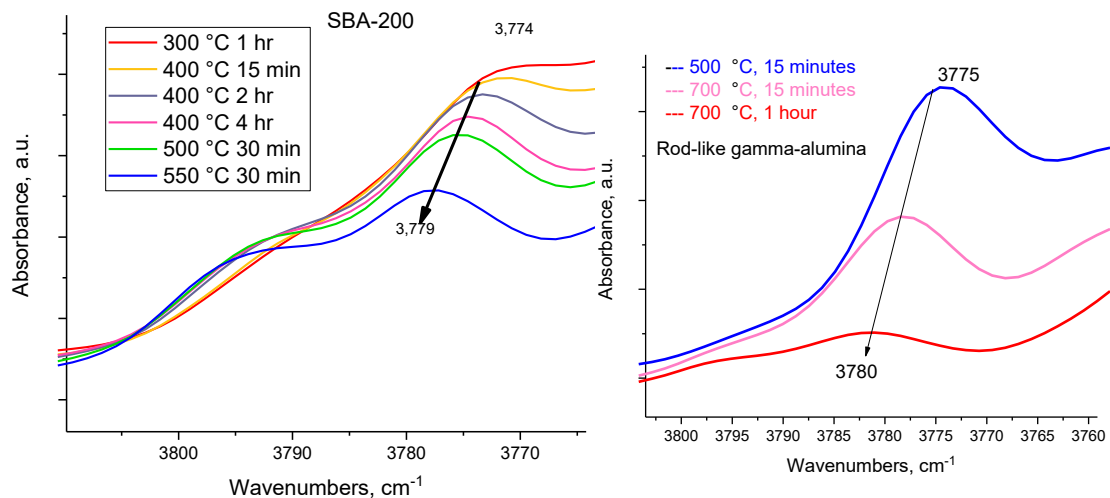
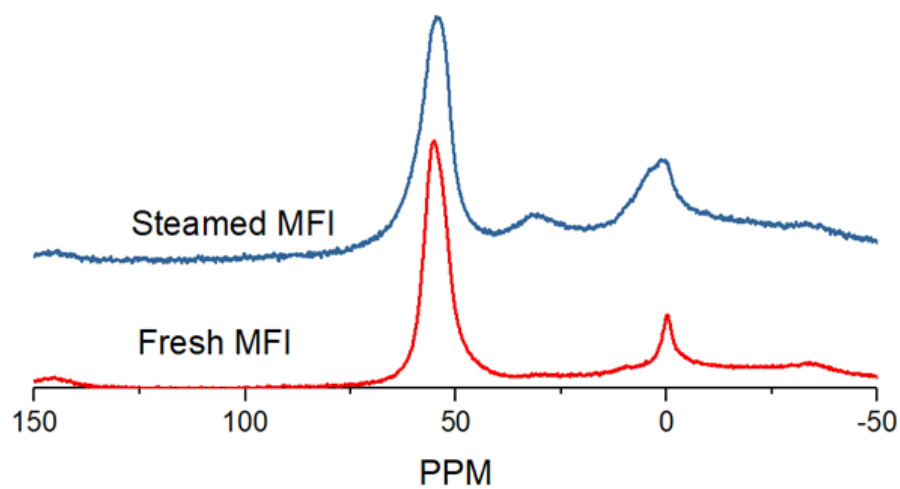


Fig. S4. FTIR of the OH region of SBA-200 and rod-like gamma-alumina samples during thermal treatments. Spectra were recorded at room temperature after specified thermal treatments.



5

Fig. S5. Solid-state ²⁷Al NMR of fresh and steamed MFI samples. The band ~ 33 ppm corresponds to penta-coordinated Al.

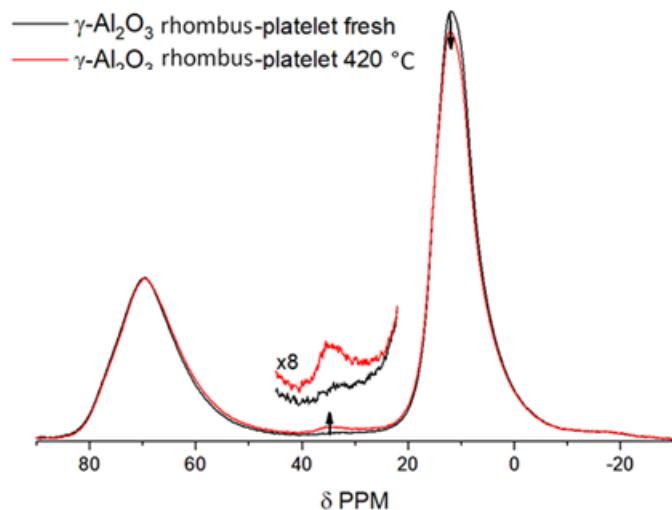


Fig. S6. Solid-state ^{27}Al NMR fresh and dehydroxylated rhombus-platelet gamma-alumina sample (SA ~ 70 m²/g). Only tetra, penta and octa-Al sites are present. Upon dehydroxylation, surface octahedral $\text{O}_5\text{Al(VI)-OH}$ sites dehydroxylate [12] and form penta-sites. Their small abundance is due to the fact that majority of Al remains in the bulk (tetra and octa-Al sites), and only a smaller fraction of Al sites resides on the surface. As the Alumina nano-particle size decreases, more and more Al surface atoms (in terms of relative surface/bulk ratio) get exposed as evidenced from Fig. S5 and discussion in the main text.

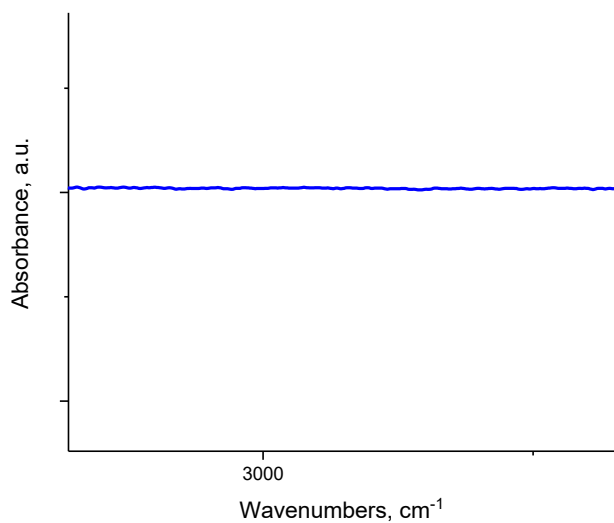


Figure S7. FTIR spectra showing the C-H stretching region of gamma-alumina that was not treated at high temperature (the sample was heated at 300 °C under vacuum for 15 minutes, this treatment is not enough to dehydroxylate $O_5Al(VI)-OH$ sites) before and after methane pulse at 200 °C.

5

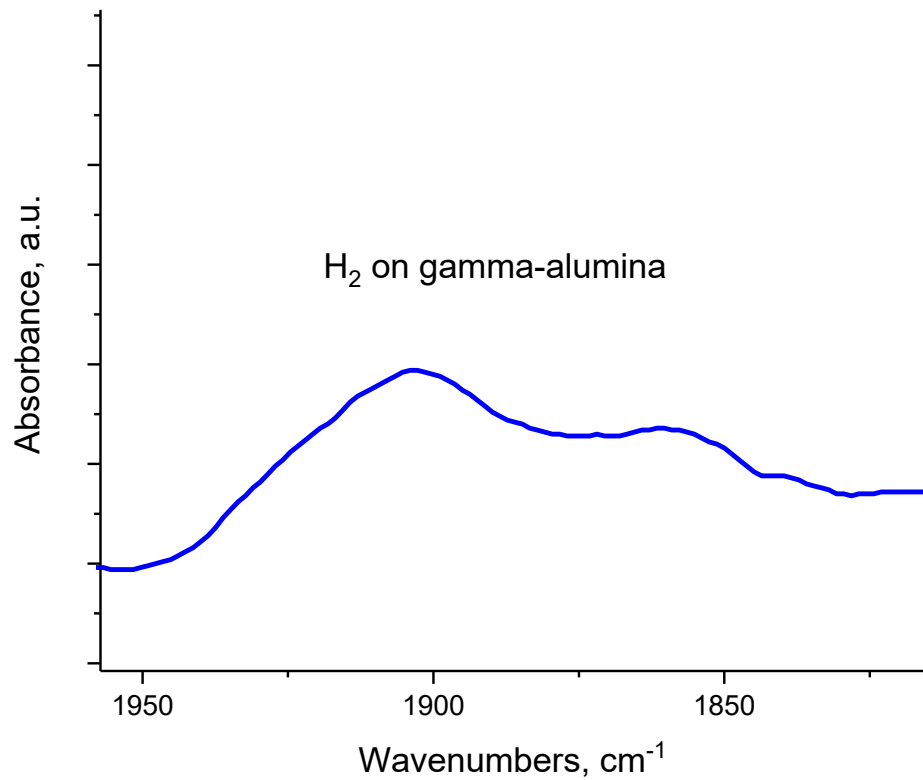


Figure S8. FTIR spectra in the Al-H stretching region after H₂ treatment of gamma-alumina (treated at 500 °C).

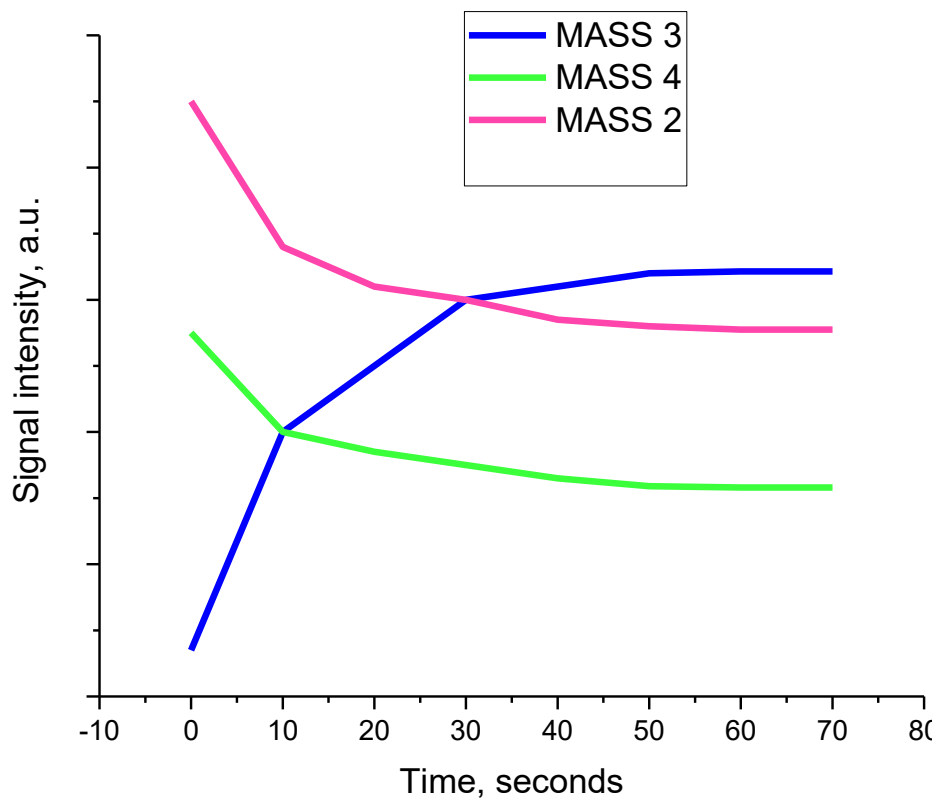


Figure S9. H_2+D_2 reaction monitored with mass-spec in static FTIR system at temperature 100 °C. A mixture of H_2+D_2 was pre-mixed in ~ 1.6-1.7 volume ratio and introduced into the infrared cell with rhombus-platelet gamma-alumina sample (dehydroxylated at 500 °C). Mass 3 corresponds to product of the reaction HD. Mass 2 corresponds to H_2 . Mass 4 corresponds to D_2 .

5